Full Paper

Applied Organometallic Chemistry

Received: 28 December 2014 Revised: 25 February 2015 Accepted: 25 February 2015 Published online in Wiley Online Library

(wileyonlinelibrary.com) DOI 10.1002/aoc.3313

Synthesis, crystal structure, electrochemistry and antioxidative activity of copper(II), manganese(II) and nickel(II) complexes containing bis(*N*-ethylbenzimidazol-2-ylmethyl)aniline

Huilu Wu*, Hongping Peng, Yanhui Zhang, Fei Wang, Han Zhang, Cuiping Wang and Zaihui Yang

Bis(*N*-ethylbenzimidazol-2-ylmethyl)aniline (Etbba) and its transition metal complexes, [Cu(Etbba)$(Cl)_2$]·DMF (1), [Mn(Etbba)$(Cl)_2$] (2) and [Ni(Etbba)$(Cl)_2$] (3), have been synthesized and characterized on the basis of elemental analysis, molar conductivity, UV–visible, infrared and NMR spectroscopies and X-ray crystallography. The coordination environment of complex 1 can be described as distorted square-based pyramidal, while complexes 2 and 3 each have a distorted trigonal bipyramidal geometry. Cyclic voltammograms of complex 1 indicate an electrochemically quasi-reversible Cu^{2+}/Cu^{+} couple. In addition, the antioxidant activities of the free ligand and its complexes were investigated using the superoxide and hydroxyl radical scavenging methods *in vitro*. Complexes 1–3 are found to possess potent hydroxyl radical scavenging activity and to be better than standard antioxidants like vitamin C and mannitol. Furthermore, complexes 1 and 2 exhibit significant superoxide radical activity.

Additional supporting information may be found in the online version of this article at the publisher's web-site.

Keywords: benzimidazole; transition metal complexes; crystal structure; electrochemical property; antioxidation

Introduction

Due to the structural versatility in coordination chemistry, the study of small-molecule chemistry of transition metal coordination assemblies is a dynamic and thriving field which has drawn ever-increasing research interests in recent decades.[1–3] The study of the structural, spectroscopic and electronic properties of metal centers present in biological systems is crucial to understand their roles in nature.[4] These centers are often modeled by using small molecules containing donor atoms that reproduce the coordination around the metal ion.[5] For this reason, the synthesis of complexes oriented to mimic metal sites of various types of metalloproteins constitutes an important branch in both inorganic and organic chemistry.[6] In this context, copper, nickel and manganese are present in a diverse group of metalloenzymes, in which the metal ions are coordinated to nitrogen atoms.[7]

Benzimidazole is a typical heterocyclic ligand with nitrogen atom as the donor atom. Interest in exploring benzimidazole derivatives and their metal complexes has been increasing since the recognition that many of these materials may serve as models which mimic both the structure and reactivity of metal sites in biological systems and can also possess a broad spectrum of biological activity.[8] Due to their privileged structure and properties,[9] benzimidazoles and their derivatives exhibit a wide variety of pharmacological activities, including antitumor,[10] antiviral,[11] anticancer,[12] antimicrobial,[13] antihypertensive[14] and anti-inflammatory or analgesic activities.[15] Moreover, as a typical heterocyclic ligand, the large benzimidazole rings not only provide potential supramolecular recognition sites for $\pi\cdots\pi$ stacking interactions, but also act as hydrogen bond acceptors and donors to assemble coordination complexes.[16]

Interest in bis(2-benzimidazolyl)aniline and its derivatives is widespread. In our previous work, we investigated the coordinating ability of various benzimidazoles.[17,18] In the present article, the synthesis, crystal structures and electrochemical properties of bis(*N*-ethylbenzimidazol-2-ylmethyl)aniline (Etbba) and three of its metal complexes are presented. The antioxidant activities (scavenging effects on $O_2^{-\bullet}$ and $OH^{-\bullet}$) of the Etbba ligand and its complexes have also been studied. Information obtained from this study will be helpful in the development of some new antioxidants.

Experimental

Materials and Methods

All chemicals and solvents were of reagent grade and used without further purification. C, H and N elemental analyses were carried out

* *Correspondence to: Huilu Wu, School of Chemical and Biological Engineering, Lanzhou Jiaotong University, Lanzhou, Gansu 730070, PR China. E-mail: wuhuilu@163.com*

School of Chemical and Biological Engineering, Lanzhou Jiaotong University, Lanzhou, Gansu, 730070, PR China

using a Carlo Erba 1106 elemental analyzer. IR spectra were recorded in the 400–4000 cm^{-1} region with a Nicolet FT-VERTEX 70 spectrophotometer using KBr pellets. Electronic spectra were obtained using a Lab-Tech UV Bluestar spectrophotometer with a spectral resolution of 0.2 nm. Absorption spectra were measured with a Spectrumlab 722sp spectrophotometer at room temperature. ^1H NMR spectra were recorded with a Varian VR 300 MHz spectrometer and ^{13}C NMR spectra with a Mercury plus 400 MHz NMR spectrometer with tetramethylsilane as internal standard and DMSO-d_6 as solvent.

Electrolytic conductance measurements were made with a DDS-307 type conductivity bridge using 3×10^{-3} mol dm^{-3} solutions in DMF at room temperature. Electrochemical measurements were performed with an LK2005A electrochemical analyzer under nitrogen at 293 K. A glassy carbon working electrode, a platinum-wire auxiliary electrode and an Ag/AgCl reference electrode ([Cl^-] = 1.0 mol l^{-1}) were used in the three-electrode measurements. The electroactive component was at a concentration of 1.0×10^{-3} mol dm^{-3} with tetrabutylammonium perchlorate (0.1 mol dm^{-3}) used as the supporting electrolyte in DMF solution. The synthetic route to the free Etbba ligand is shown in Scheme 1.

Synthesis of Compounds

Synthesis of Etbba

The precursor bba was synthesized according to the procedure reported previously.[18,19] The Etbba ligand was synthesized using a method analogous to the literature method.[18] Yield 61.3%; m.p. 240–242°C. Anal. Calcd for $C_{26}H_{27}N_5$ (%): C, 76.25; H, 6.65; N, 17.10. Found (%): C, 76.35; H, 6.50; N, 17.15. IR (KBr; ν, cm^{-1}): 745 ν(o-Ar), 1268 ν(C–N), 1460 ν(C=N), 1599 ν(C=C). ^1H NMR (300 MHz, $CDCl_3$, δ, ppm): 7.73 (d, J = 7.3 Hz, 4H, H11′), 7.22 (d, J = 7.3 Hz, 4H, H12′), 7.10–6.90 (m, 5H, Ar–H), 4.87 (s, 2H, $-CH_2-$N), 4.05–4.16 (m, 4H, $-CH_2-$Me), 1.21–1.28 (m, 6H, $-CH_3$). ^{13}C NMR (400 MHz, DMSO-d_6, δ, ppm): 153.85 (C4), 147.22 (C6), 138.54 (C10), 134.14 (C9) 129.13 (C2), 122.84 (C12), 119.36 (C1), 115.59 (C11), 113.47 (C3), 50.10 (C5), 34.60 (C7), 18.70 (C8). UV–visible (in DMF, λ_{max}, nm): 280, 286. Molar conductance (Λ_M, DMF solution, 297 K): 3 S cm^2 mol^{-1}.

Preparation of complexes

Three complexes were prepared using a similar procedure. To a stirred solution of ligand Etbba (0.5 mmol, 204.7 mg) in hot EtOH (10 ml) was added a solution of metal chloride salt (0.50 mmol: $CuCl_2{\cdot}4H_2O$, 85.24 mg; $MnCl_2{\cdot}2H_2O$, 98.96 mg; $NiCl_2{\cdot}6H_2O$, 118.8 mg) in EtOH (10 ml). The sediment generated rapidly. The precipitate was filtered off, washed with ethanol and absolute diethyl ether, and dried *in vacuo*. The dried precipitate was dissolved in DMF to form a solution into which diethyl ether was allowed to diffuse at room temperature. Crystals suitable for X-ray measurement were obtained after several days.

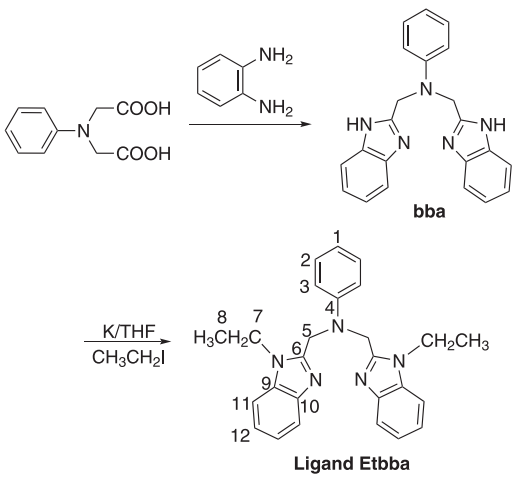

Scheme 1. Synthesis of the Etbba ligand.

Complex **1**. Yield 68%. Anal. Calcd for $C_{29}H_{34}Cl_2CuN_6O$ (%): C, 56.45; H, 5.55; N, 13.62. Found (%): C, 56.40; H, 5.58; N, 13.66. IR (KBr; ν, cm^{-1}): 750 ν(o-Ar), 1293 ν(C–N), 1452 ν(C=N), 1620 ν(C=C). UV–visible (DMF, λ_{max}, nm) (ε_{max} ($l\,mol^{-1}\,cm^{-1}$)): 275 (1.60×10^4), 281 (1.54×10^4), 777 (286). Molar conductance (Λ_M, DMF): 13 S cm^2 mol^{-1}.

Complex **2**. Yield 70%. Anal. Calcd for $C_{26}H_{27}Cl_2MnN_5$ (%): C, 58.33; H, 5.08; N, 13.08. Found (%): C, 58.35; H, 5.10; N, 13.06. IR (KBr; ν, cm^{-1}): 761 ν(o-Ar), 1267 ν(C–N), 1453 ν(C=N), 1601 ν(C=C). UV–visible (DMF, λ_{max}, nm) (ε_{max} ($l\,mol^{-1}\,cm^{-1}$)): 279 (1.59×10^4), 285 (1.49×10^4). Molar conductance: (Λ_M, DMF): 21 S cm^2 mol^{-1}.

Complex **3**. Yield 81%. Anal. Calcd for $C_{26}H_{27}Cl_2N_5Ni$ (%): C, 57.92; H, 5.05; N, 12.99. Found (%): C, 57.90, H, 5.06; N, 13.00. IR (KBr; ν, cm^{-1}): 759 ν(o-Ar), 1267 ν(C–N), 1454 ν(C=N), 1595 ν(C=C). UV–visible (DMF, λ_{max}, nm) (ε_{max} ($l\,mol^{-1}\,cm^{-1}$)): 275 (1.55×10^4), .282 (1.43×10^4), 773 (4.73). Molar conductance (Λ_M, DMF): 40 S cm^2 mol^{-1}.

Antioxidant Activities

Hydroxyl radical scavenging activity

Hydroxyl radicals were generated in aqueous medium through the Fenton-type reaction.[20,21] Stock solutions (3×10^{-3} M) of the compounds were prepared in absolute DMF. The reaction mixture (3 ml) contained 1.0 ml of 0.10 mmol aqueous safranin, 1 ml of 1.0 mmol aqueous EDTA–Fe(II), 1 ml of 3% aqueous H_2O_2 and a series of quantitative microadditions of solutions of the test compound. A sample without the test compound was used as the control. The reaction mixtures were incubated at 37°C for 30 min in a water bath. The scavenging effect for $OH^{-\bullet}$ was calculated from the following expression:

$$\text{Scavanging effect}\ (\%) = \frac{A_{\text{sample}} - A_{\text{blank}}}{A_{\text{control}} - A_{\text{blank}}} \times 100$$

where A_{sample} is the absorbance of the sample in the presence of the test compound, A_{blank} is the absorbance of the blank in the absence of the test compound and $A_{control}$ is the absorbance in the absence of the test compound and EDTA–Fe(II).[22]

Superoxide radical scavenging activity

Test solutions were prepared by diluting stock solution with DMF. A non-enzymatic system containing 0.5 ml of 3.3×10^{-5} M vitamin B_2, 1 ml of 2.3×10^{-4} M nitrotetrazolium blue chloride (NBT), 1 ml of 0.05 M methionine (MET) and 2.5 ml of 0.02 M phosphate buffer (Na_2HPO_4–NaH_2PO_4, pH = 7.8) was used to produce the superoxide anion ($O_2^{-\bullet}$), and the scavenging rate of $O_2^{-\bullet}$ under the influence of 0.3–3.0 μM of the test compound was determined by monitoring the reduction in rate of transformation of NBT to monoformazan dye.[23] The solutions of MET, vitamin B_2 and NBT were prepared in 0.02 M phosphate buffer (pH = 7.8) avoiding light. The reactions were monitored at 560 nm with a UV–visible spectrophotometer, and the rate of absorption change was determined. The

percentage inhibition of NBT reduction was calculated using the following equation[24]:

$$\text{Inhibition of NBT reduction } (\%) = \left(1 - k'/k\right) \times 100$$

where k' and k are the slopes of the straight lines of absorbance values as a function of time in the presence and absence of superoxide dismutase (SOD) mimic compound, respectively. The IC_{50} values for the complexes were determined by plotting the graph of percentage inhibition of NBT reduction against the concentration of the complex. The concentration of the complex which causes 50% inhibition of NBT reduction is reported as IC_{50}.

X-Ray Crystallography

Diffraction intensities for complexes **1–3** were collected using a Bruker Smart CCD diffractometer with graphite-monochromated Mo K_α radiation ($\lambda = 0.71073$ Å) at 296(2) K. Data reduction and cell refinement were performed using the SMART and SAINT programs.[25] The structure was solved by direct methods and refined by full-matrix least-squares against F^2 of data using SHELXTL software.[26] All H atoms attached to C atoms except for DMF groups were fixed geometrically and treated as riding with C–H = 0.93 or 0.97 Å with $U_{iso}(H) = 1.2U_{eq}(C)$. All H atoms attached to N atoms were fixed geometrically and treated as riding with N–H = 0.86 Å with $U_{iso}(H) = 1.2U_{eq}(N)$. Crystal data and details of the refinement for complexes **1–3** are given in Table 1. Selected bond lengths and angles are presented in Table 2.

Table 2. Selected bond distances (Å) and angles (°) for complexes **1-3**

Complex **1**			
Cu1–N3	1.9668(16)	Cu1–N5	1.9729(16)
Cu1–Cl1	2.2534(7)	Cu1–Cl2	2.2999(6)
Cu1–N1	2.5320(16)		
N3–Cu1–N5	149.07(7)	N3–Cu1–Cl1	99.26(5)
N5–Cu1–Cl1	99.30(5)	N3–Cu1–Cl2	94.56(5)
N5–Cu1–Cl2	94.06(5)	Cl1–Cu1–Cl2	126.41(3)
N3–Cu1–N1	74.91(6)	N5–Cu1–N1	75.33(6)
Cl1–Cu1–N1	111.61(4)	Cl2–Cu1–N1	121.99(4)
Complex **2**			
Mn1–N3	2.165(3)	Mn1–N5	2.179(2)
Mn1–Cl1	2.3312(18)	Mn1–Cl2	2.3865(17)
Mn1–N1	2.669(3)		
N3–Mn1–N5	110.11(8)	N3–Mn1–Cl1	111.64(8)
N5–Mn1–Cl1	123.52(7)	N3–Mn1–Cl2	105.34(8)
N5–Mn1–Cl2	99.32(9)	Cl1–Mn1–Cl2	104.39(6)
N3–Mn1–N1	69.85(9)	N5–Mn1–N1	71.11(9)
Cl1–Mn1–N1	89.62(7)	Cl2–Mn1–N1	165.93(5)
Complex **3**			
Ni1–N3	2.024(3)	Ni1–N5	2.054(3)
Ni1–Cl2	2.2732(12)	Ni1–Cl1	2.3125(11)
Ni1–N1	2.351(3)		
N3–Ni1–N5	111.01(12)	N3–Ni1–Cl2	101.78(10)
N5–Ni1–Cl2	140.90(9)	N3–Ni1–Cl1	102.19(9)
N5–Ni1–Cl1	95.24(9)	Cl2–Ni1–Cl1	98.14(4)
N3–Ni1–N1	76.47(10)	N5–Ni1–N1	77.46(11)
Cl2–Ni1–N1	90.54(8)	Cl1–Ni1–N1	171.30(8)

Results and Discussion

The synthetic route to the free Etbba ligand is shown in Scheme 1. The complexes were prepared by reaction of the Etbba ligand with $CuCl_2{\cdot}4H_2O$, $MnCl_2{\cdot}2H_2O$ or $NiCl_2{\cdot}6H_2O$ in ethanol. All compounds are stable under atmospheric conditions. They are soluble in polar aprotic solvents such as DMF, DMSO and MeCN, slightly soluble in ethanol, water, ethyl acetate and chloroform, and insoluble in Et_2O and petroleum ether. The molar conductivities of complexes **1–3** in DMF solution indicate that they are non-electrolytes.

Table 1. Crystal and structure refinement data for complexes **1–3**

	1	**2**	**3**
Molecular formula	$C_{29}H_{34}Cl_2CuN_6O$	$C_{26}H_{27}Cl_2MnN_5$	$C_{26}H_{27}Cl_2N_5Ni$
Molecular weight	617.06	535.37	539.14
Crystal system	Monoclinic	Monoclinic	Monoclinic
Space group	$P2_1/c$	$P2_1/n$	$P2_1/n$
a (Å)	9.0532(9)	12.929(13)	12.617(2)
b (Å)	14.5584(15)	14.076(14)	14.524(3)
c (Å)	22.421(2)	4.464(14)	14.132(3)
β (°)	92.917(10)	103.504(11)	104.600(2)
V (Å^3)	2951.2(5)	2559(4)	2506.3(8)
Z	4	4	4
D (calculated; g cm^{-3})	1.389	1.389	1.429
F(000)	1284	1108	1120
Crystal size (mm)	0.30 × 028 × 0.24	0.29 × 0.25 × 0.21	0.29 × 0.26 × 0.23
θ range for data collection (°)	1.7 to 25.5	1.9 to 25.5	1.9 to 25.5
Reflections collected	19 897	17 205	16 978
Independent reflections	5441 ($R_{int} = 0.022$)	4741 ($R_{int} = 0.035$)	4662 ($R_{int} = 0.079$)
Data/restraints/parameters	5441/0/356	4741/0/309	4662/0/309
Goodness-of-fit on F^2	1.05	1.04	1.02
Reflections with $I > 2\sigma(I)$	4587	3535	2825
Final R_1, wR_2 indices ($I > 2\sigma(I)$)	$R_1 = 0.030$, $wR_2 = 0.078$	$R_1 = 0.035$, $wR_2 = 0.088$	$R_1 = 0.046$, $wR_2 = 0.092$
R_1, wR_2 indices (all data)	$R_1 = 0.039$, $wR_2 = 0.083$	$R_1 = 0.055$, $wR_2 = 0.099$	$R_1 = 0.098$, $wR_2 = 0.111$

IR and UV–Visible Spectra

The IR spectral data for the complexes along with their assignments are given in Table 3. In the spectrum of the free ligand, a strong band is found around 1268 cm^{-1} along with another less strong band around 1460 cm^{-1}. By analogy with the spectrum of imidazole, the former is attributed to ν(C–N) and the latter to ν(C=N).[27,28] The first shifts by about 20 cm^{-1} and the second by about 7 cm^{-1} in the spectra of the complexes, which implies direct coordination of the imine nitrogen atoms to the metal. These are the preferred nitrogen atoms for coordination, as found in other metal complexes with benzimidazoles.[29] This fact agrees with the X-ray diffraction results (see below).

DMF solutions of the Etbba ligand and its complexes show, as expected, almost identical UV spectra. The UV bands of Etbba (279, 286 nm) are only marginally blue-shifted (2–5 nm) in the spectra of the complexes, which is evidence of C=N coordination to the metal center. These bands are assigned to $n \rightarrow \pi^*$ and $\pi \rightarrow \pi^*$ (imidazole) transitions.[30,31] Complexes **1** and **3** exhibit one absorption band, which is assigned to $d \rightarrow d$ transition.

Description of Structures

*Crystal structure of complex **1***

The ORTEP representation of the structure of complex **1**, including atom numbering scheme, is shown in Fig. 1 and selected bond lengths and bond angles are listed in Table 2. The asymmetric unit comprises neutral [Cu(Etbba)Cl_2] and a DMF molecule. The Cu(II) center is five coordinate within a Cl_2N_3 chromophore. The Etbba ligand acts as a tridentate N-donor, and two chloride atoms complete the coordination. The coordination of the Cu(II) atom may be best described as distorted square-based pyramidal ($\tau = 0.38$). The parameter τ is defined as $(\beta - \alpha)/60$ (where β = N3–Cu1–N5, α = Cl1–Cu1–Cl2) and its value varies from 0 (in regular square-pyramidal geometry) to 1 (trigonal bipyramidal).[32] This geometry is assumed by the Cu(II) center so as to relieve steric crowding. The equatorial plane is occupied by two N atoms of the Etbba ligand and two chloride anions. The axial position is occupied by N1, with Cu1–N1 of 2.5320(16) Å being the longest Cu–N bond (Table 2).

Table 3. IR bands (cm^{-1}) of compounds

Compound	$\nu_{(Ar)}$	$\nu_{(C-N)}$	$\nu_{(C=N)}$	$\nu_{(C=C)}$
Etbba	745	1268	1460	1599
1	750	1293	1452	1620
2	761	1267	1453	1601
3	759	1267	1454	1613

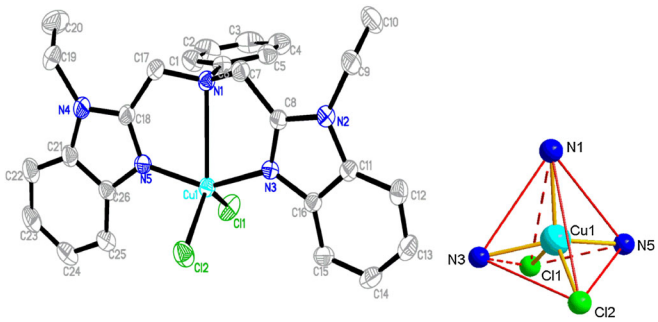

Figure 1. Molecular structure and atom numberings of complex **1** with hydrogen atoms omitted for clarity.

*Crystal structure of complex **2***

The metal atom in **2** (Fig. 2) is coordinated within a Cl_2N_3 donor set as for **1** but the coordination geometry more resembles distorted trigonal bipyramidal ($\tau = 0.70$).[32] The axial sites are occupied by N1 and Cl2, with Cl2–Mn1–N1 = 165.93(5)°. The trigonal plane is occupied by the two ligating N atoms of the benzimidazolyl groups and a chloride atom, namely atoms N3/N5/Cl1.

*Crystal structure of complex **3***

In complex **3** (Fig. 3), a similar mode of coordination of Etbba is found as described for **1** and **2**. The coordination geometry is intermediate between the extremes with $\tau = 0.51$.[33]

Electrochemical Studies

The electrochemical properties of the three complexes were studied using cyclic voltammetry in DMF. Only complex **1** exhibits a pair of cathodic and anodic waves. The data are collected in Table 4 and an example voltammogram is shown in Fig. 4. The separation between the cathodic and anodic peak potentials, ΔE_p, and the current i_{pa}/i_{pc} indicate a quasi-reversible redox process assignable to the Cu(II)/Cu(I) couple.[34] The neutral free Etbba ligand proves not to be electroactive over the range −1.2 to +1.2 V.

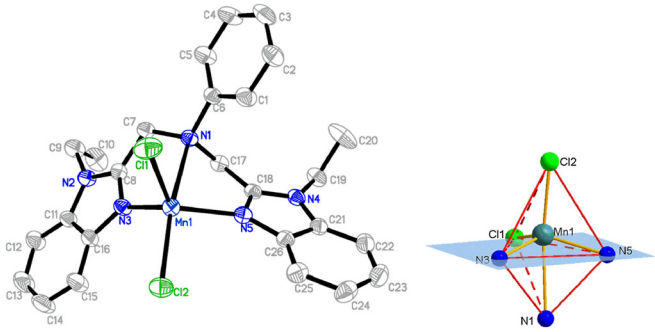

Figure 2. Molecular structure of complex **2** with hydrogen atoms omitted for clarity.

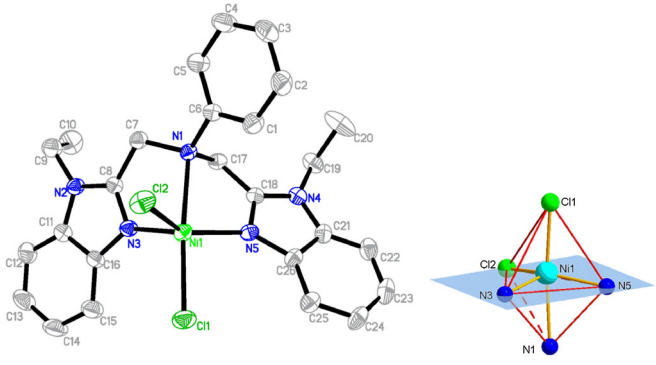

Figure 3. Molecular structure of complex **3** showing displacement ellipsoids at the 30% probability level. Hydrogen atoms have been omitted for clarity.

Table 4. Electrochemical data for complex **1**[a]

Complex	E_{pc}	E_{pa}	ΔE_p	$E_{1/2}$	i_{pa}	i_{pc}	I
1	0.2748	0.3815	0.1067	0.32815	3.3	4.9	0.675

[a] $\Delta E = E_{pa} - E_{pc}$; $E_{1/2} = (E_{pa} + E_{pc})/2$; scan rate = 0.05 V s^{-1}; $I = i_{pa}/i_{pc}$.

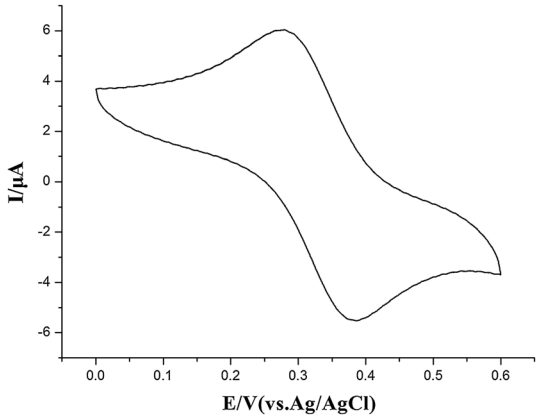

Figure 4. Cyclic voltammogram of complex **1** recorded with a platinum electrode in DMF solution containing tetrabutylammonium perchlorate (0.1 M).

According to previous reports,[35] a transition metal complex must have a redox potential below 0.65 V ($E°(O_2–O_2^-)$) and above −0.33 V ($E°(O_2–O_2^-)$) in order to be an effective mimic of SOD, so toxic singlet oxygen cannot be formed. The redox potential of 0.1067 V shows that complex **1** has SOD activity.

Antioxidant Activities

Generation of reactive oxygen species is a normal process in the life of aerobic organisms. $OH^{-\bullet}$ and $O_2^{-\bullet}$ are two clinically important reactive oxygen species in the human body.[36] They are produced in most organ systems and participate in various physiological and pathophysiological processes such as carcinogenesis, aging, viral infection, inflammation and others.[37] Consequently, in this paper, the ligand Etbba and its complexes were studied for their antioxidant activity by comparing their scavenging effects on $OH^{-\bullet}$ and $O_2^{-\bullet}$.

Hydroxyl radical scavenging activity

We first compared the abilities of the present compounds to scavenge hydroxyl radicals with those of the well-known natural antioxidants mannitol and vitamin C, using the same method as reported in a previous paper.[17,38] The 50% inhibitory concentration (IC_{50}) values of mannitol and vitamin C are about 9.6×10^{-3} and 8.7×10^{-3} M, respectively. Figure 5 shows plots of hydroxyl radical scavenging effect (%) for Etbba and its complexes. The IC_{50} values of complexes **1**, **2** and **3** are $(5.61 \pm 0.045) \times 10^{-6}$, $(8.21 \pm 0.069) \times 10^{-5}$ and $(9.28 \pm 0.022) \times 10^{-5}$ M, respectively; Etbba does not have activity. The results indicate that the hydroxyl radical scavenging activity of three complexes follows the order **1** > **2** > **3**, which implies that these complexes exhibit

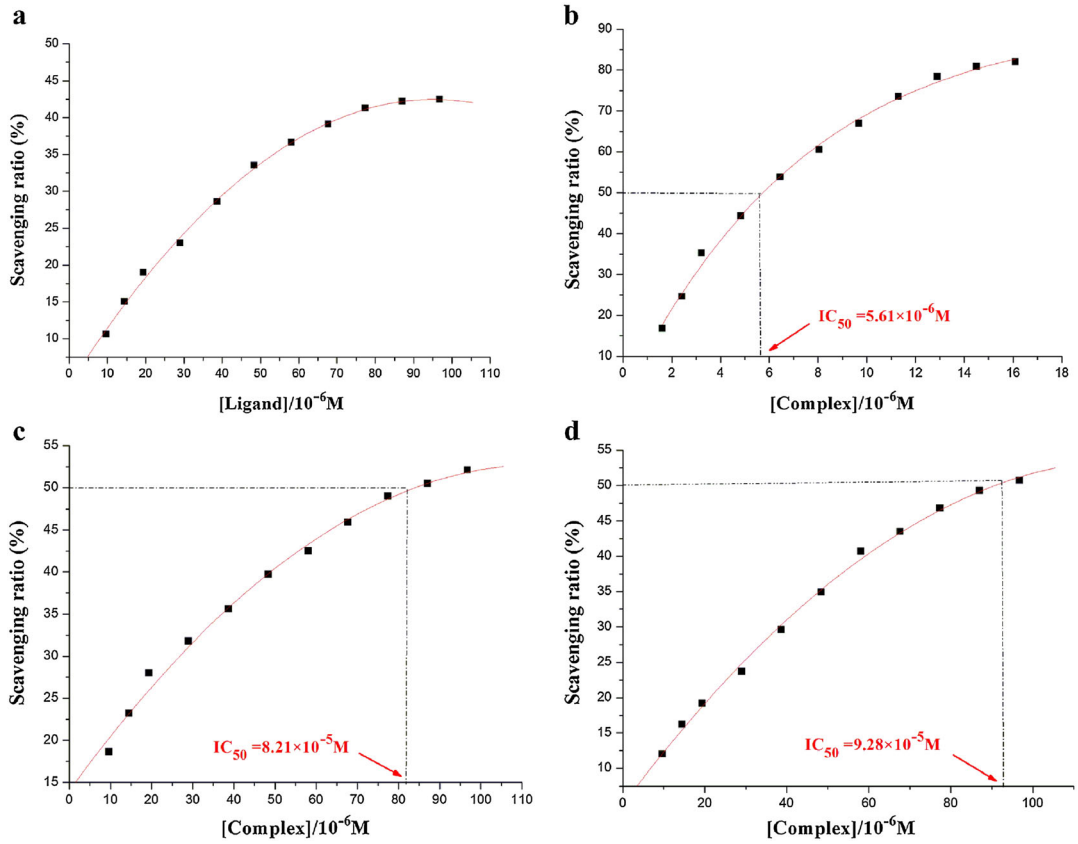

Figure 5. Inhibitory effect of (a) Etbba, and complexes (b) **1**, (c) **2** and (d) **3** on $OH^{-\bullet}$ radicals; the suppression ratio increases with increasing concentration of the test compounds.

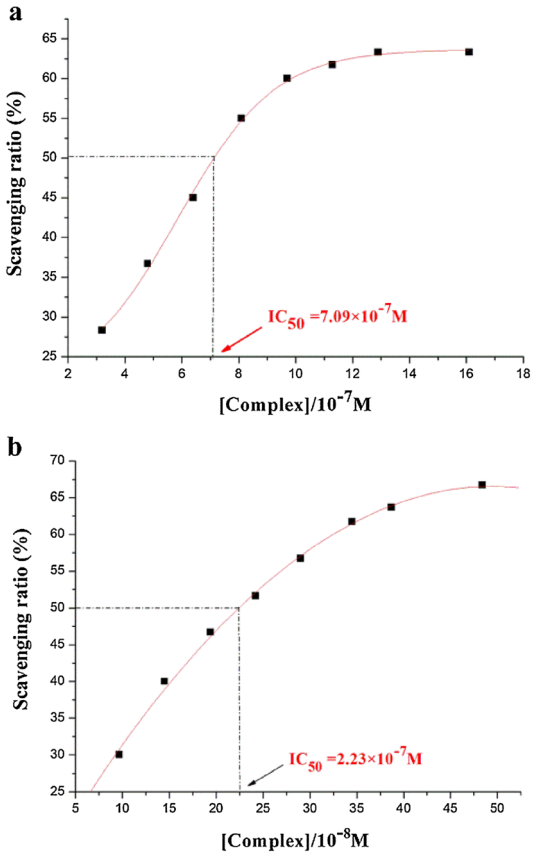

Figure 6. Superoxide radical scavenging effect for complexes (a) **2** and (b) **1**.

better scavenging activity than mannitol and vitamin C. The lower IC_{50} values observed in antioxidant assays demonstrate **1–3** have potential to be applied as scavengers to eliminate radicals.

Superoxide radical scavenging activity

As a significant assay of antioxidant activity, the superoxide radical ($O_2^{-\bullet}$) scavenging activity of **1–3** has been investigated.[39] As can be seen from Fig. 6, the IC_{50} values are $(2.23 \pm 0.081) \times 10^{-7}$ and $(7.09 \pm 0.037) \times 10^{-7}$ M for complexes **1** and **2**, respectively. Therefore, **1** and **2** demonstrate good SOD activities with respect to the standard SOD mimic manganese complexes (EUK-8 $IC_{50} = 1.3 \times 10^{-6}$ M and EUK-189 $IC_{50} = 1.4 \times 10^{-6}$ M)[40] and the standard SOD mimic copper complex ($IC_{50} = 2.6 \times 10^{-5}$ M)[41]; **3** does not have activity. We find that the order of the suppression ratio of the tested compounds for $O_2^{-\bullet}$ is **1** > **2**, consistent with the electrochemical studies. The result indicates that complexes **1** and **2** exhibit good superoxide radical scavenging activity and may be inhibitors to scavenge $O_2^{-\bullet}$ *in vivo* which merits further investigation.

Conclusions

The Etbba ligand and its complexes have been synthesized and characterized. The geometries of **1–3** were analyzed through single-crystal X-ray diffraction and shown to have Cl_2N_3 donor sets. The coordination environment of the Cu(II) atom in **1** can be described as distorted square-based pyramidal, while the geometric structure of **2** may be considered distorted trigonal bipyramidal, with **3** having an intermediate coordination geometry. Electrochemical studies show quasi-reversible redox behavior for **1**. Furthermore, **1–3** exhibit good hydroxyl radical scavenging activity, and **1** and **2** display excellent antioxidant activity for superoxide radical. These findings clearly indicate that transition metal complexes with benzimidazole have many potential applications, which warrants further *in vivo* experiments and perhaps pharmacological assays.

Acknowledgments

This research was supported by the National Natural Science Foundation of China (grant no. 21367017), the Fundamental Research Funds for the Gansu Province Universities (212086), Natural Science Foundation of Gansu Province (grant no. 1212RJZA037) and 'Qing Lan' Talent Engineering Funds for Lanzhou Jiaotong University.

References

[1] N. L. Rosi, J. Kim, M. Eddaoudi, B. Chen, M. O'Keeffe, O. M. Yaghi, *J. Am. Chem. Soc.* **2005**, *127*, 1504.
[2] H. Zheng, E. Q. Gao, Z. M. Wang, C. H. Yan, M. Kurmoo, *Inorg. Chem.* **2005**, *44*, 862.
[3] J. Fan, H. F. Zhu, T. Okamura, W. Y. Sun, W. X. Tang, N. Ueyama, *Chem. Eur. J.* **2003**, *9*, 4724.
[4] S. Leininger, B. Olenyuk, P. J. Stang, *Chem. Rev.* **2000**, *100*, 853.
[5] E. Bouwman, J. Reedijk, *Coord. Chem. Rev.* **2005**, *249*, 1555.
[6] X. C. Huang, Y. Y. Lin, J. P. Zhang, X. M. Chen, *Angew. Chem. Int. Ed.* **2006**, *45*, 1557.
[7] A. Tamayo, J. Casabó, L. Escriche, P. González, C. Lodeiro, A. C. Rizzi, C. D. Brondino, M. C. G. Passeggi, R. Kivekals, R. Sillanpala, *Inorg. Chem.* **2007**, *46*, 5665.
[8] S. X. Wang, S. Y. Yu, Q. H. Luo, Q. Y. Wang, J. Q. Shi, Q. J. Wu, *Transition Met. Chem.* **1994**, *19*, 205.
[9] D. A. Horton, G. T. Bourne, M. L. Smythe, *Chem. Rev.* **2003**, *103*, 893.
[10] E. Lukevics, P. Arsenyan, I. Shestakova, I. Domracheva, A. Nesterova, O. Pudova, *Eur. J. Med. Chem.* **2001**, *36*, 507.
[11] L. Garuti, M. Roberti, E. D. Clercq, *Bioorg. Med. Chem. Lett.* **2002**, *12*, 2707.
[12] A. Gellis, H. Kovacic, N. Boufatah, P. Vanelle, *Eur. J. Med. Chem.* **2008**, *43*, 1858.
[13] Ö. Ö. Guven, T. Erdogan, H. Goker, S. Yildiz, *Bioorg. Med. Chem. Lett.* **2007**, *17*, 2233.
[14] K. Kopanska, A. Najda, Z. Justyna, L. Chomicz, J. Piekarczyk, P. Myjak, M. Bretner, *Bioorg. Med. Chem.* **2004**, *12*, 2617.
[15] S. M. Sondhi, S. Rajvanshi, M. Johar, N. Bharti, A. Azam, A. K. Singh, *Eur. J. Med. Chem.* **2002**, *37*, 835.
[16] H. Y. Liu, H. Wu, J. Yang, Y. Y. Liu, B. Liu, Y. Y. Liu, J. F. Ma, *Cryst. Growth Des.* **2011**, *11*, 2920.
[17] H. L. Wu, J. K. Yuan, Y. Bai, G. L. Pan, H. Wang, J. Kong, X. Y. Fan, H. M. Liu, *Dalton Trans.* **2012**, *41*, 8829.
[18] H. L. Wu, B. Liu, F. Kou, F. Jia, J. K. Yuan, Y. Bai, *J. Chin. Chem. Soc. Taip.* **2012**, *5*, 836.
[19] R. Cariou, J. J. Chirinos, V. C. Gibson, G. Jacobsen, A. K. Tomov, G. J. P. Britovsek, A. J. P. White, *Dalton Trans.* **2010**, *39*, 9039.
[20] R. Barbehenn, T. Dodick, U. Poopat, B. Spencer, *Arch. Insect Biochem. Physiol.* **2005**, *60*, 32.
[21] C. P. Tan, J. Liu, L. M. Chen, S. Shi, L. N. Ji, *J. Inorg. Biochem.* **2008**, *102*, 1644.
[22] Z. Y. Guo, R. E. Xing, S. Liu, H. H. Yu, P. B. Wang, C. P. Li, P. C. Li, *Bioorg. Med. Chem. Lett.* **2005**, *15*, 4600.
[23] X. Y. Le, S. R. Liao, X. P. Liu, X. L. Feng, *J. Coord. Chem.* **2006**, *59*, 985.
[24] Q. H. Luo, Q. Lu, A. B. Dai, L. G. Huang, *J. Inorg. Biochem.* **1993**, *51*, 655.
[25] Bruker, *APEX2, SAINT*, Bruker AXS Inc., Madison, **2006**.
[26] G. M. Sheldrick, *Acta Crystallogr. A* **2008**, *64*, 112.
[27] H. L. Wu, H. C. Huang, J. K. Yuan, F. Kou, G. S. Chen, B. B. Jia, Y. Yang, Y. L. Lan, *Z. Naturforsch.* **2010**, *65b*,1334.
[28] R. Bakshi, P. Mathur, *Inorg. Chim. Acta* **2010**, *363*, 3477.
[29] F. Z. C. Fellah, J. P. Costes, C. Duhayon, J. C. Daran, J. P. Tuchagues, *Polyhedron* **2010**, *29*, 2111.

[30] H. L. Wu, J. K. Yuan, Y. Bai, G. L. Pan, H. Wang, X. B. Shu, *J. Photochem. Photobiol. B* **2012**, *107*, 65.
[31] E. Suresh, M. M. Bhadbhade, D. Srinivas, *Polyhedron* **1996**, *15*, 4133.
[32] S. Youngme, J. Phatchimkun, U. Sukangpanya, C. Pakawatchai, N. Chaichit, P. Kongsaeree, J. Krzystek, B. Murphy, *Polyhedron* **2007**, *26*, 871.
[33] H. L. Wu, H. Wang, X. L. Wang, G. L. Pan, F. R. Shi, Y. H. Zhang, Y. C. Bai, J. Kong, *New J. Chem.* **2014**, *38*, 1052.
[34] A. W. Addison, H. M. J. Hendriks, J. Reedije, L. . K. Thompson, *Inorg. Chem.* **1981**, *20*, 103.
[35] H. L. Wu, R. R. Yun, K. T. Wang, K. Li, X. C. Huang, T. Sun, Y. Y. Wang, *Z. Anorg. Allg. Chem.* **2010**, *636*, 1397.
[36] A. Banerjee, N. Dasgupta, B. De, *Food Chem.* **2005**, *90*, 727.
[37] M. Xu, Y. C. Zhang, Z. H. Xu, Z. Z. Zeng, *Inorg. Chim. Acta* **2012**, *384*, 324.
[38] T. R. Li, Z. Y. Yang, B. D. Wang, D. D. Qin, *Eur. J. Med. Chem.* **2008**, *43*, 1688.
[39] B. D. Wang, Z. Y. Yang, P. Crewdson, D. D. Wang, *J. Inorg. Biochem.* **2007**, *101*, 1492.
[40] O. Iranzo, *Bioorg. Chem.* **2011**, *39*, 73.
[41] R. N. Patel, D. K. Patel, V. P. Sondhiya, K. K. Shukla, Y. Singh, A. Kumar, *Inorg. Chim. Acta* **2013**, *405*, 209.

Supporting Information

Additional supporting information may be found in the online version of this article at the publisher's web-site.